

1 **Highlights**

- 2 ✓ We generated mice and cells that express ferritin-mKate2 under *Arc* promoter control.
- 3 ✓ *Arc* promoter activity was increased in the neurons after pilocarpine treatment.
- 4 ✓ An increase in T2-weighted image signal was found in the neurons.
- 5 ✓ We successfully visualized *Arc* promoter-driven neuronal activities by MRI.

6

7 **Abstract**

8 Visualization of direct neuronal activity to understand brain function is one of the most
9 important challenges in neuroscience. We have previously demonstrated that in vivo and in
10 vitro gene expression of the ferritin reporter system could be detected by magnetic
11 resonance imaging (MRI). In addition, increased neuronal activity induces *Arc*, an
12 immediate early gene, and insertion of a destabilized fluorescent reporter dVenus under *Arc*
13 promoter control has been used for monitoring neuronal activities in the brain by optical
14 imaging. In this study, to visualize *Arc* promoter-driven neuronal activities directly, we
15 generated transgenic mice and cell lines that express a destabilized fusion reporter
16 ferritin-mKate2 under *Arc* promoter control. When transgenic mice and cell lines were
17 treated with pilocarpine, a non-selective muscarinic agonist, an increase in T2-weighted
18 image signal was successfully found in neuronal cells. There was a difference in peak time
19 between MRI and fluorescence imaging, which might result from the binding process of iron
20 with ferritin. Visualization of *Arc* promoter-driven neuronal activity is essential to understand

- 1 neural mechanisms underlying cognitive processes and complex behaviors, and could be a
- 2 useful tool for therapeutic approaches in the brain by MRI.
- 3 **Keywords:** Magnetic resonance imaging, ferritin, neuronal activity, *Arc* promoter,
- 4 non-invasive imaging, gene expression

1 Introduction

2 Visualization of direct neuronal activity to understand brain function is an important
3 challenge in neuroscience. Magnetic resonance imaging (MRI) is a standard tool for
4 non-invasive imaging without radiation because it provides high resolution images with good
5 contrast between different tissues. Functional magnetic resonance imaging (fMRI) is a
6 popular technique to map brain activity in a particular area of the brain and it is widely used
7 for basic research and clinical diagnosis. However, neural activities are indirectly monitored
8 by fMRI; fMRI detects signal changes in blood oxygenation and flow and they are correlated
9 with changes in neural activity [1], but it remains unclear whether observation by fMRI is
10 similar with observation of direct neuronal activity in brain function.

11 Previously, we demonstrated that the ferritin reporter system can be used to detect in vivo
12 and in vitro gene expression [2]. Ferritin is an iron storage metalloprotein and encapsulates
13 iron derivatives up to 4500 iron atoms [3]. Ferritin consists of heavy and light chains, and
14 ferritin heavy chains can bind to iron derivatives. Because iron derivatives are often used for
15 contrast reagents in MRI [4], accumulation of endogenous iron increases T2-weighted signal,
16 which results in the image becoming darker. Therefore, if ferritin heavy chains are used as a
17 reporter for neuronal activity-related gene expression, neuronal activity may be visualized in
18 MRI.

1 In the mammalian brain, expression of *Arc* (also known as *Arg3.1*), an immediate early gene,
2 is induced by increased neuronal activity [5,6] and associated with various brain functions
3 including learning, memory, and emotion. Insertion of a destabilized fluorescent reporter
4 dVenus under *Arc* promoter control was used to monitor neuronal activities in the brain by
5 optical imaging [7]. We postulated that expression of a ferritin reporter under the *Arc*
6 promoter could be used to visualize neuronal activities by MRI based on gene expression.
7 In order to visualize the expression dynamics of the *Arc* gene in vitro and in vivo, we
8 designed a vector capable of expressing ferritin heavy chain and a destabilized mKate2
9 fusion protein (ferritin-mKate2) reporter under *Arc* promoter control. We generated
10 *Arc*-ferritin-mKate2 (AFM) mice and an N18_AFM neuronal cell line using the vector and
11 visualized *Arc* promoter-driven neuronal activities after pilocarpine treatment by MRI.

1 **Materials and Methods**

2 *Arc-ferritin-mKate2 (AFM) mice*

3 pferritin-mKate2 plasmids were made from a pmKate2-N vector [8] (Evrogen Joint Stock
4 Company, Moscow, Russia) by insertion of the mouse ferritin heavy chain sequence
5 (NM_010239) at a multi-cloning site. Polymerase chain reaction mutagenesis was used to
6 delete the stop codon from the mKate2 gene. The stop codon-deleted mKate2 gene was
7 fused in-frame to the degradation signal sequence of pGL3 (R2.2)-Basic (Promega,
8 Madison, WI, USA), which comprises the CL1 and PEST protein degradation signal motifs,
9 as well as an AU-rich mRNA degradation element. The 7.1 kb of the *Arc* promoter region
10 was isolated from the mouse genomic DNA derived from the BAC clone (RP23-459I23,
11 Thermo Fisher Scientific, Waltham, MA, USA). For the generation of the AFM construct, the
12 *Arc* promoter, a synthetic intron (nucleotide residues 766-1005 of pRL-TK, Promega), and
13 the ferritin-mKate2 gene were subcloned immediately upstream of the SV40
14 polyadenylation signal of pGL3-Basic (Promega). The AFM construct was used for
15 pronuclear microinjection of fertilized eggs of BDF1 (C57BL/6 × DBA/2) mice. Fourteen
16 founder lines were obtained and one line, which showed highest levels of mKate2
17 expression in preliminary experiments, was chosen for establishment of transgenic lines.
18 Further studies were conducted using offspring obtained from mating the transgenic mice

1 with C57BL/6 mice. To examine *Arc* promoter-driven neuronal activities, AFM mice were
2 treated with pilocarpine, a non-selective muscarinic receptor agonist, which induced *Arc*
3 gene expression in neurons in a previous study [9]. In brief, mice were injected with
4 methylscopolamine (1 mg/kg i.p. in saline) 15 min before intraperitoneal pilocarpine injection
5 followed by injection of pilocarpine (300 mg/kg i.p. in saline). Behavior was observed for 15
6 min after the injection and scored as described previously [10]. Mice showing tonic-clonic
7 convulsion (score 4) were chosen, temporally observed using MRI, and sacrificed at 0, 1, 4,
8 and 24 h after pilocarpine treatment. More than four AFM mice were sacrificed at each time
9 point. C57BL/6 mice were used as control experiment.

10 *N18 transfected with AFM construct (N18_AFM) cells*

11 N18 cells (1×10^6 cells/400 μ l), a mouse neuronal clone, were mixed with 10 μ g of AFM
12 construct in a 4 mm gap cuvette. The cuvette was set in an ECM830 electroporator (BTX
13 Instrument Division Harvard Apparatus, Holliston, MA, USA) and electroporation was
14 performed under the following conditions (LV mode, 170 V, 70 ms pulse length, single pulse).
15 A single clone was picked up after limiting dilutions and propagated for this study. N18_AFM
16 cells were cultured in Eagle's Minimum Essential Medium (MEM) (Sigma-Aldrich, St Louis,
17 MO, USA) supplemented with 10% fetal bovine serum, 1% non-essential amino acid
18 solution (Sigma-Aldrich), 1 mM sodium pyruvate (Sigma-Aldrich), and 1%

1 penicillin-streptomycin (Thermo Fisher Scientific) in a 95% air/5% CO₂-humidified
2 atmosphere. N18_AFM cells were plated on a 100 mm Cell Culture Dish at a density of 1.0
3 × 10⁶ cells and were cultivated for 72 h. Cells were treated with 200 μM ferric nitrate and
4 stimulated with 1 μM pilocarpine at 0, 1, 4, and 24 h before harvest. Cells were washed with
5 PBS twice and harvested using trypsin-EDTA (0.25%) (Thermo Fisher Scientific). Cells were
6 collected in 0.2 ml tubes for fluorescent and MRI.

7 *Fluorescent observation and immunohistochemical analysis*

8 Brains were isolated from sacrificed AFM mice. mKate2 fluorescence from the brains and
9 cell pellets was observed using an optical imager Maestro (PerkinElmer, Waltham, MA USA)
10 with liquid crystal tunable filters (LCTF) that could distinguish between mKate2 and intrinsic
11 fluorescence. Brains were embedded in OCT compounds (Sakura Finetek Japan, Tokyo,
12 Japan) and freshly frozen at −80 °C. Serial frozen sections (10 μm) were cut on a cryostat,
13 transferred to MAS coated slide glass (Matsunami Glass Ind., Osaka, Japan), and
14 immediately air-dried. Sections were fixed with 4% paraformaldehyde in PBS (pH 7.2) at
15 room temperature for 15 min. Sections were permeated with 0.1% triton-X in PBS and
16 blocked with a blocking buffer (1% bovine serum albumin, 10% normal goat serum, and
17 0.05% sodium azide) for 1 h at room temperature. The sections were labeled with polyclonal
18 antibodies against ferritin (Abcam, Cambridge, UK) or MAP-2 (Cell Signaling Technology,

1 Danvers, MA, USA) at a dilution of 1:200 for 1 h at room temperature. Then, the sections
2 were visualized with Alexa Fluor 488 conjugated goat anti-rabbit IgG (Thermo Fisher
3 Scientific) at a dilution of 1:500 and counterstained with Hoechst 33342 (Thermo Fisher
4 Scientific) at a dilution of 1:1000. Fluorescent images were taken on a microscope equipped
5 with a unique fluorescent camera Nuance2 (PerkinElmer), which also contained LCTF and
6 could distinguish among Alexa Fluor 488 fluorescence, mKate2 fluorescence, and
7 autofluorescence. Fluorescent images were analyzed using Maestro software
8 (PerkinElmer).

9 *Magnetic resonance imaging (MRI)*

10 T2-weighted images were obtained from brains of AFM mice and cell pellets of N18_AFM
11 cells. The mice were lightly anesthetized using 1.5% isoflurane and images were collected
12 on a 1T MRI (MRTechnology, Tsukuba, Japan). In brief, the parameters were as follows: T2
13 sequences with a TR/TE of 3000/69 ms, field of view of 30, and two averages were taken for
14 a total acquisition time of about 14 min. Signal intensity in the region of interest was
15 analyzed from images using ImageJ software.

16 *Western blotting*

17 Minced brain was lysed in RIPA buffer (20 mM Tris-HCl, pH 7.5, 1% NP-40, 0.15 M NaCl, 1
18 mM EDTA, 1 μ g/ml leupeptin) on ice and sonicated using a Bioruptor (Cosmo Bio, Tokyo,

1 Japan) for 5 min before BCA protein assay (Thermo Fisher Scientific), which was performed
2 to determine protein concentrations according to the manufacturer's instructions. Twenty
3 micrograms of total protein per sample was aliquoted, mixed with loading buffer (Cell
4 Signaling Technology), boiled for 5 min, and separated by SDS-PAGE on 12.5% minigels
5 (Oriental Instruments, Kanagawa, Japan). Separated proteins were then transferred to
6 PVDF membranes on an iBlot Gel Transfer Device (Thermo Fisher Scientific) and blocked in
7 5% nonfat dry milk (Cell Signaling Technology)/TBS (Tris buffered saline)-0.1% Tween at
8 room temperature for 1 h. To detect ferritin and mKate2, membranes were incubated with
9 polyclonal antibodies against ferritin (Abcam) or RFP (Thermo Fisher Scientific) at a dilution
10 of 1:5000 at 4 °C overnight. On the following day, membranes were washed with TBS-0.1%
11 Tween three times, and incubated with HRP conjugated goat anti-rabbit IgG antibodies in
12 5% nonfat dry milk/TBS-0.1% Tween at a dilution of 1:5000 at room temperature for 1 h.
13 Protein was visualized by chemiluminescence using ECL Clarity (Bio-rad, Hercules, CA,
14 USA) and Light Capture II (Atto, Tokyo, Japan). In order to normalize for sample loading and
15 protein transfer, the membranes were stripped with Stripping Solution (Wako Pure
16 Chemicals Industries, Osaka, Japan) and reprobed with monoclonal antibodies against
17 GAPDH (Wako Pure Chemicals Industries) at a dilution of 1:2000 as indicated. Molecular
18 weight and signal intensity were analyzed using CS Analyzer software (Atto).

1 *Measurement of intracellular iron concentration*

2 Intracellular iron concentration in cell pellets of N18_AFM cells was measured using an iron
3 assay kit (Iron Assay kit LS – Ferrozine method, Metallogenetics Co., Ltd., Chiba, Japan)
4 according to the manufacturer's instructions. In brief, 5×10^6 cells were homogenized in cell
5 lysis buffer (50 mM Tris-HCl (pH8.0), 150 mM NaCl, 0.1% SDS, 0.5% sodium deoxycholate,
6 1% TritonX-100) and sonicated using a Bioruptor (Cosmo Bio). Hydrochloric acid (6M) was
7 added to the lysates for a final concentration of 0.01 M (pH>2). The lysates were then mixed
8 well and incubated for 30 min at room temperature. After the lysates were centrifuged at
9 $20000 \times g$ for 15 min at 4 °C, the supernatants were used as samples for the iron assay kit
10 based on the ferrozine method [11]. Intracellular iron concentration was determined by
11 measurement of the absorbance at 540 nm using an iMark Microplate Absorbance Reader
12 (Bio-rad) and corrected using the protein concentration by BCA protein assay (Thermo
13 Fisher Scientific).

14 *Statistical analysis*

15 Numerical values are the mean +/- SD. Each experiment was repeated more than three
16 times. Statistical significance was evaluated using one-way ANOVA and Dunnett's post hoc
17 test. Differences were considered significant when the *P* value was less than 0.05.

18

1 Results

2 To visualize *Arc* promoter-driven neuronal activities, *Arc*-ferritin-mKate2 (AFM) mice were
3 treated with pilocarpine and analyzed by MRI (Figure 1A). Four hours after injection of
4 pilocarpine, the T2-weighted image signal intensity in hippocampus and cortex but not
5 cerebellum was significantly increased and returned to baseline by 24 h. To confirm whether
6 *Arc* promoter activity was induced by pilocarpine treatment, we examined mKate2
7 fluorescence in the brain (Figure 1B). The increase in mKate2 fluorescence peaked at 1 h
8 and then returned to baseline by 24 h in the hippocampus and the cortex, but no change in
9 mKate2 fluorescence was found in the cerebellum. In the hippocampus,
10 immunohistochemical analysis showed that the highest mKate2 expression was found in
11 dentate granule cells and pyramidal cells in CA1-3 regions 1 h after pilocarpine treatment
12 (Figure 2A). In addition, mKate2-expressing cells were co-localized with expression of
13 ferritin (Figure 2B) and MAP-2 (Figure 2C), which was a specific marker for neuronal cells.
14 To understand the reporter dynamics in the brain, expression of ferritin-mKate2 fusion
15 protein after pilocarpine treatment was analyzed by western blotting (Figure 2D). In the
16 cortex and hippocampus, expression of ferritin-mKate2 fusion protein peaked at 1 h and
17 gradually decreased by 24 h, whereas expression of endogenous ferritin was unchanged.
18 To clarify whether ferritin protein induced in neuronal cells served as an MRI reporter for

1 neuronal activities, the cell pellet from the N18_AFM neuronal cell line, which expressed
2 ferritin-mKate2 fusion protein under control of the *Arc* promoter, was analyzed by MRI and
3 optical imaging after pilocarpine treatment (Figure 3A and 3B). T2-weighted image signal
4 intensity in the cell pellet was significantly increased 4 h after pilocarpine treatment and
5 returned to baseline by 24 h (Figure 3A), whereas mKate2 red fluorescence peaked at 1 h
6 and returned to baseline by 24 h (Figure 3B) similar to that in the AFM mouse brain. To
7 understand whether the increase in T2-weighted image signal was dependent on binding
8 between ferritin and iron, the iron concentration in the cell pellet was measured (Figure 3C).
9 The increase in iron concentration peaked 4 h after pilocarpine treatment and returned to
10 baseline by 24 h similar to the results of the MRI observation.

11

1 Discussion

2 In this study, we demonstrated that *Arc* promoter-driven neuronal activities were visualized
3 in MRI as well as optical imaging using a ferritin-mKate2 fusion reporter. When AFM mice
4 were treated with pilocarpine, expression of ferritin-mKate2 fusion protein drastically and
5 transiently increased and then recovered to baseline in the hippocampus and cortex, which
6 are brain regions confirmed to have an increase of *Arc* expression in previous studies [12].
7 In addition, we could hardly find alteration in T2-weighted image signal from
8 pilocarpine-treated C57BL/6 mice and vehicle-treated AFM mice as shown in Figure 1A.
9 These indicate that the increase in T2-weighted image signal from pilocarpine-treated AFM
10 mice does not arise from alteration of blood flow and edema after pilocarpine treatment.
11 Several types of muscarinic acetylcholine receptors are expressed in the hippocampus and
12 cortex [13]. Moreover, N18 cells express muscarinic acetylcholine receptors and respond to
13 muscarinic agonists [14,15], so that our imaging results might indicate direct and indirect
14 induction of *Arc* in activated neurons by pilocarpine, a non-selective muscarinic agonist.
15 There was a gap in peak time between MRI and optical imaging *in vivo* and *in vitro*.
16 Expression of ferritin-mKate2 fusion protein peaked 1 h after pilocarpine treatment, whereas
17 the increase in signal intensity of the T2-weighted image peaked at 4 h. In addition, the
18 concentration of intracellular iron in N18_AFM cells also peaked 4 h after pilocarpine

1 treatment. These results suggested that it takes time for iron to bind the ferritin-mKate2
2 fusion protein. Previously, we showed that the ferritin signal was significantly enhanced in
3 iron-permeated cells compared to that of non-permeated cells [2]. Transferrin receptors
4 have an important role in transporting iron from extracellular fluid to intracellular fluid [16]. In
5 addition, a recent study showed that transferrin receptor overexpression was effective for
6 transporting iron and as an MR reporter [17]. Therefore, co-expression of transferrin
7 receptors with ferritin might reduce the gap in peak times between MRI and optical imaging.
8 Furthermore, ferritin expression in the extracellular space of the plasma membrane instead
9 on the cytoplasmic side may also decrease the difference in peak times.

10 Alternatively, the gap between peak times may be related to the formation of ferritin subunit
11 complex. Ferritin consists of 24 subunits, which contain both heavy and light chains. The
12 heavy chain facilitates iron uptake and the light chain is involved in protein stability and iron
13 mineralization [18]. One ferritin molecule, a complex of heavy and light chains, can bind to a
14 maximum of 4500 iron atoms [3]. In this study, we overexpressed ferritin heavy chain under
15 *Arc* promoter control. Therefore, the ratio between the complex and the ferritin heavy chain
16 alone might have temporally changed after pilocarpine treatment.

17 In conclusion, a ferritin reporter under control of an *Arc* promoter provides another
18 alternative to visualize *Arc* promoter-driven neuronal activity using MRI. MRI is a useful,

1 non-invasive, and safe tool for basic research and clinical diagnosis because it does not use
2 radiation to obtain high resolution tomographic images. Visualization of *Arc* promoter-driven
3 neuronal activity by MRI is essential to understand neural mechanisms underlying cognitive
4 process and complex behaviors, and maybe have potential as a useful tool for therapeutic
5 approaches to the brain.

1 **Acknowledgements**

2 This study was partly supported by the Research Foundation for Development of System
3 and Technology for Advanced Measurement and Analysis, System development type from
4 Japan Science and Technology Agency (JST-SENTAN Program).

5

6 The authors declare no conflicts of interest.

1 **References**

- 2 [1] S. Ogawa, D.W. Tank, R. Menon, J.M. Ellermann, S.G. Kim, H. Merkle, K. Ugurbil,
3 Intrinsic signal changes accompanying sensory stimulation: Functional brain mapping
4 with magnetic resonance imaging, *Proc. Natl. Acad. Sci. U. S. A.* 89 (1992) 5951–5955.
5 doi:10.1073/pnas.89.13.5951.
- 6 [2] K. Ono, K. Fuma, K. Tabata, M. Sawada, Ferritin reporter used for gene expression
7 imaging by magnetic resonance., *Biochem Biophys Res Commun.* 388 (2009) 589–594.
8 <http://www.ncbi.nlm.nih.gov/pubmed/19683514>.
- 9 [3] E.C. Theil, Ferritin: at the crossroads of iron and oxygen metabolism., *J. Nutr.* 133 (2003)
10 1549S–53S. doi:10.1016/s0304-4157(96)00014-7.
- 11 [4] H.-J. Weinmann, W. Ebert, B. Misselwitz, H. Schmitt-Willich, Tissue-specific MR contrast
12 agents, *Eur. J. Radiol.* 46 (2003) 33–44. doi:10.1016/S0720-048X(02)00332-7.
- 13 [5] W.W. Link, U.U. Konietzko, G.G. Kauselmann, M.M. Krug, B.B. Schwanke, U.U. Frey,
14 D.D. Kuhl, Somatodendritic expression of an immediate early gene is regulated by
15 synaptic activity., *Proc. Natl. Acad. Sci. U. S. A.* 92 (1995) 5734–5738.
16 doi:10.1073/pnas.92.12.5734.
- 17 [6] D. Liu, D. Bei, H. Parmar, A. Matus, Activity-regulated, cytoskeleton-associated protein
18 (Arc) is essential for visceral endoderm organization during early embryogenesis, *Mech.*
19 *Dev.* 92 (2000) 207–215. doi:10.1016/S0925-4773(99)00340-8.
- 20 [7] M. Eguchi, S. Yamaguchi, In vivo and in vitro visualization of gene expression dynamics
21 over extensive areas of the brain, *Neuroimage.* 44 (2009) 1274–1283.
22 doi:10.1016/j.neuroimage.2008.10.046.
- 23 [8] D. Shcherbo, E.M. Merzlyak, T. V. Chepurnykh, A.F. Fradkov, G. V Ermakova, E.A.
24 Solovieva, K.A. Lukyanov, E.A. Bogdanova, A.G. Zaraisky, S. Lukyanov, D.M. Chudakov,
25 Bright far-red fluorescent protein for whole-body imaging, *Nat. Methods.* 4 (2007) 741–
26 746. doi:10.1038/nmeth1083.
- 27 [9] I. Teber, R. Köhling, E.-J. Speckmann, A. Barnekow, J. Kremerskothen, Muscarinic
28 acetylcholine receptor stimulation induces expression of the activity-regulated
29 cytoskeleton-associated gene (ARC)., *Brain Res. Mol. Brain Res.* 121 (2004) 131–136.
30 doi:10.1016/j.molbrainres.2003.11.017.
- 31 [10] R.S. Morrison, H.J. Wenzel, Y. Kinoshita, C. a Robbins, L. a Donehower, P. a
32 Schwartzkroin, Loss of the p53 tumor suppressor gene protects neurons from
33 kainate-induced cell death, *J. Neurosci.* 16 (1996) 1337–1345.
34 <http://www.jneurosci.org/cgi/reprint/16/4/1337%5Cnpapers2://publication/uuid/016691CA>
35 -AE28-4230-9469-B18A78330D6A.

- 1 [11] L.L. Stookey, Ferrozine-A New Spectrophotometric Reagent for Iron, *Anal. Chem.* 42
2 (1970) 779–781. doi:10.1021/ac60289a016.
- 3 [12] G.L. Lyford, K. Yamagata, W.E. Kaufmann, C.A. Barnes, L.K. Sanders, N.G. Copeland,
4 D.J. Gilbert, N.A. Jenkins, A.A. Lanahan, P.F. Worley, Arc, a growth factor and
5 activity-regulated gene, encodes a novel cytoskeleton-associated protein that is enriched
6 in neuronal dendrites, *Neuron*. 14 (1995) 433–445. doi:10.1016/0896-6273(95)90299-6.
- 7 [13] F.P. Bymaster, P.A. Carter, M. Yamada, J. Gomeza, J. Wess, S.E. Hamilton, N.M.
8 Nathanson, D.L. McKinzie, C.C. Felder, Role of specific muscarinic receptor subtypes in
9 cholinergic parasympathomimetic responses, in vivo phosphoinositide hydrolysis, and
10 pilocarpine-induced seizure activity, *Eur. J. Neurosci.* 17 (2003) 1403–1410.
11 doi:10.1046/j.1460-9568.2003.02588.x.
- 12 [14] B.K. Atwood, J. Lopez, J. Wager-Miller, K. Mackie, A. Straiker, Expression of G
13 protein-coupled receptors and related proteins in HEK293, AtT20, BV2, and N18 cell lines
14 as revealed by microarray analysis, *BMC Genomics.* 12 (2011) 14.
15 doi:10.1186/1471-2164-12-14.
- 16 [15] H. Matsuzawa, M. Nirenberg, Receptor-mediated shifts in cGMP and cAMP levels in
17 neuroblastoma cells., *Proc. Natl. Acad. Sci. U. S. A.* 72 (1975) 3472–3476.
18 doi:10.1073/pnas.72.9.3472.
- 19 [16] A.E. Deans, Y.Z. Wadghiri, L.M. Bernas, X. Yu, B.K. Rutt, D.H. Turnbull, Cellular MRI
20 contrast via coexpression of transferrin receptor and ferritin, *Magn. Reson. Med.* 56
21 (2006) 51–59. doi:10.1002/mrm.20914.
- 22 [17] S.M. Pereira, A. Herrmann, D. Moss, H. Poptani, S.R. Williams, P. Murray, A. Taylor,
23 Evaluating the effectiveness of transferrin receptor-1 (TfR1) as a magnetic resonance
24 reporter gene, *Contrast Media Mol. Imaging.* 11 (2016) 236–244.
25 doi:10.1002/cmml.1686.
- 26 [18] P. Rucker, F.M. Torti, S. V. Torti, Role of H and L subunits in mouse ferritin, *J. Biol. Chem.*
27 271 (1996) 33352–33357. doi:10.1074/jbc.271.52.33352.
28

1 **Figure legends**

2 Fig. 1 MRI and fluorescent observation of brains from pilocarpine-treated AFM mice.

3 (A) T2-weighted images from AFM mice after pilocarpine treatment were obtained by MRI.

4 The percentage increase in the T2-weighted image signal was measured and the results are

5 summarized in graphs. AFM_Vehicle; vehicle-treated AFM mice, AFM_Pilocarpine,

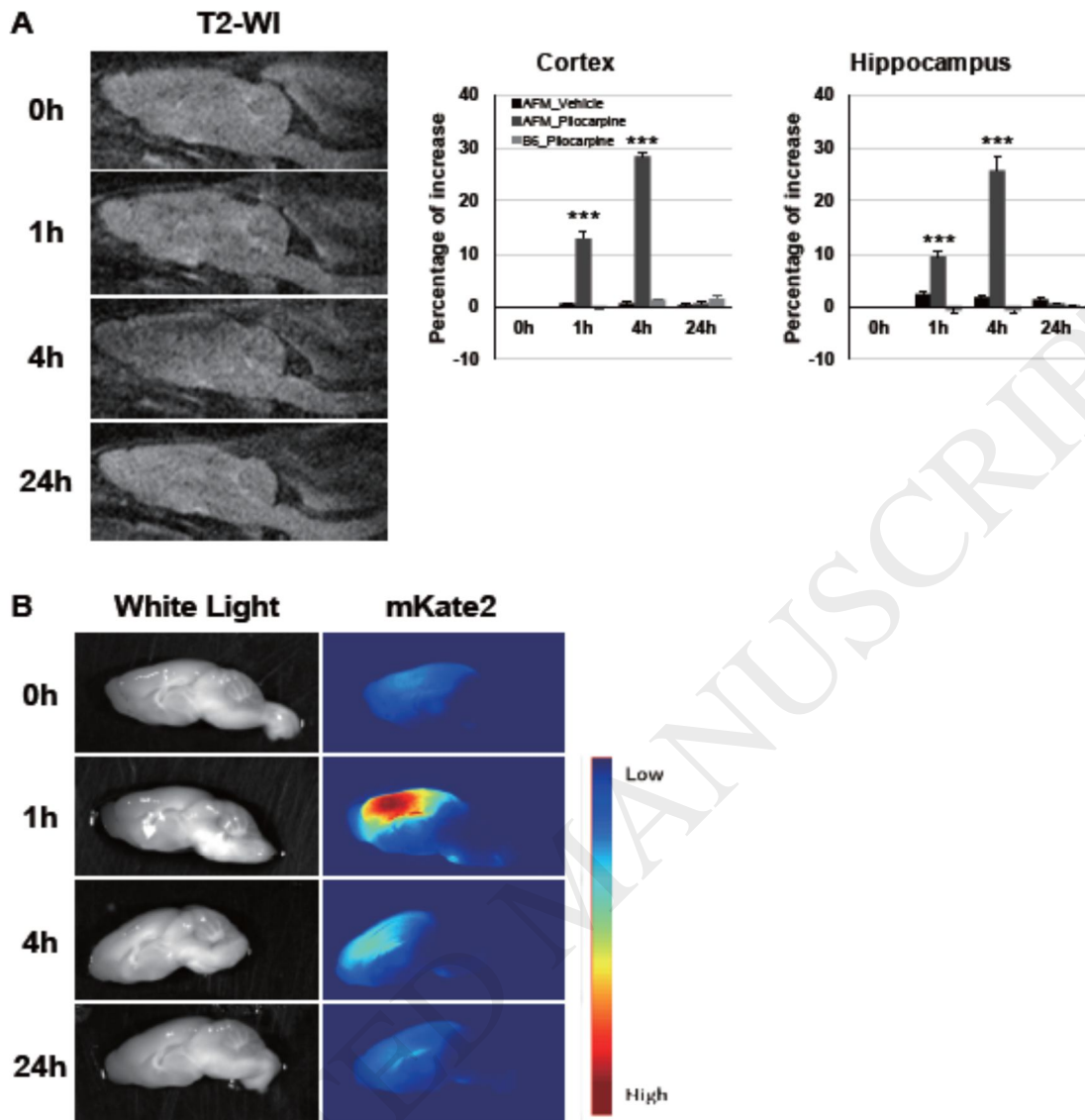
6 pilocarpine-treated AFM mice, B6_Pilocarpine; pilocarpine-treated C57BL/6 mice. $***P <$

7 0.001 compared to that at 0 h. (B) The brains from AFM mice after pilocarpine treatment

8 were observed using an optical imager Maestro. The photographs on the left show

9 observation under bright field illumination and the photographs on the right show mKate2

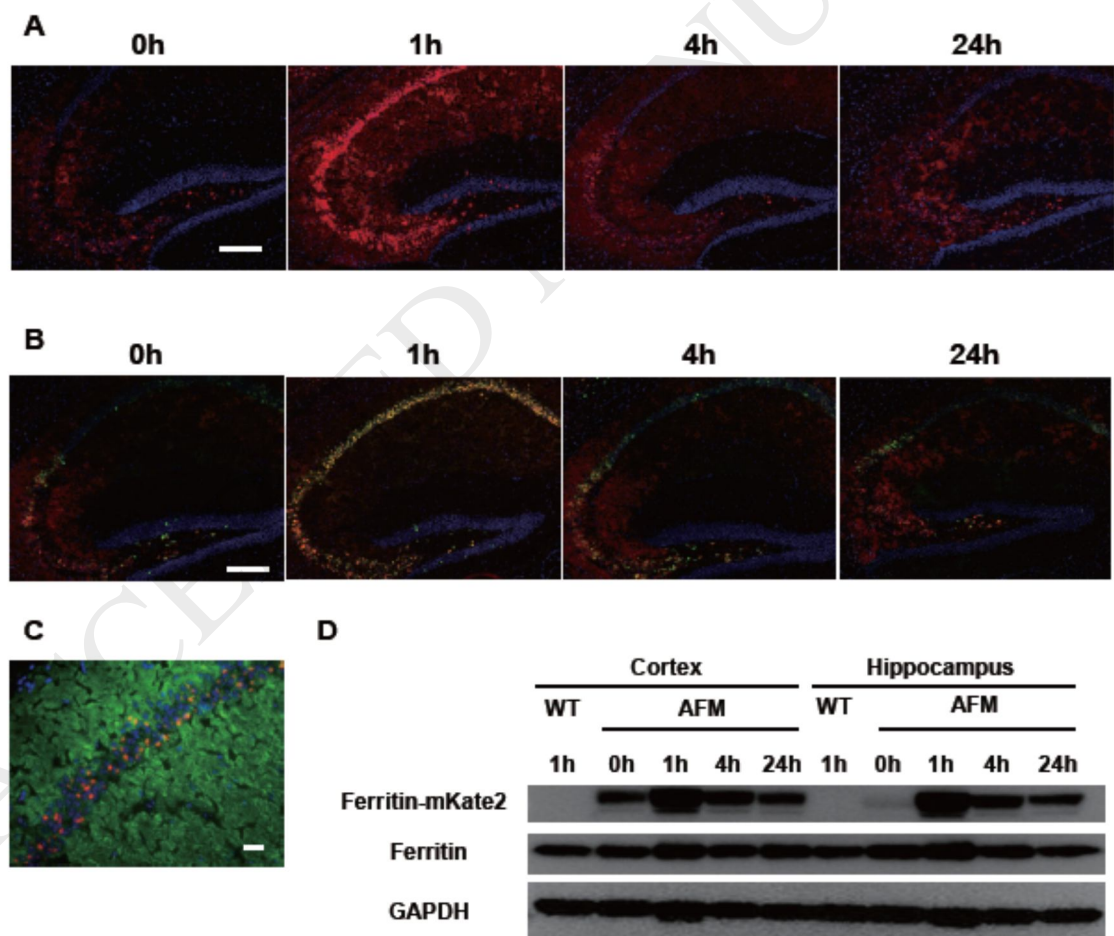
10 fluorescent images.



1
2
3
4
5 Fig. 2 Expression of ferritin-mKate2 fusion protein in AFM mice brains after pilocarpine
6 treatment.

7 (A) The photographs show mKate2 fluorescence in hippocampus at 0, 1, 4, and 24 h after

1 pilocarpine treatment. Scale bar indicates 100 μm . (B) The photographs show expression of
 2 mKate2 (red) and ferritin (green) in the hippocampus after pilocarpine treatment. Scale bar
 3 indicates 100 μm . (C) The photographs show that MAP-2 expressing neuronal cells (green)
 4 in pyramidal cell layer express mKate2 (red) 1 h after pilocarpine treatment. Scale bar
 5 indicates 20 μm . Nuclei were counterstained with Hoechst33342 (blue). (D) Expression of
 6 ferritin-mKate2 fusion protein and endogenous ferritin in the cortex and hippocampus at 0, 1,
 7 4, and 24 h after pilocarpine treatment was analyzed by Western blotting.



8

9

1

2

3 Fig. 3 MRI and fluorescent observation of N18_AFM cells after pilocarpine treatment.

4 (A) T2-weighted images from N18_AFM cells after pilocarpine treatment were temporally

5 obtained by MRI. The percentage increase in the T2-weighted image signal was measured

6 and the results are summarized in a graph. $*P < 0.05$, $**P < 0.01$ compared to that at 0 h. (B)

7 The photographs show mKate2 fluorescence in N18_AFM cell pellets after pilocarpine

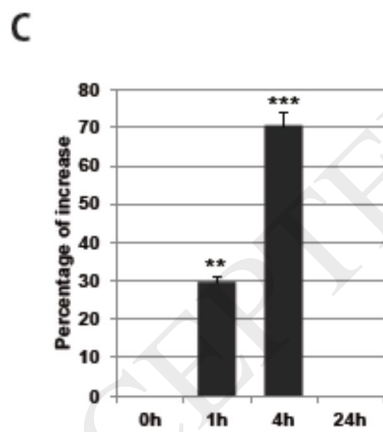
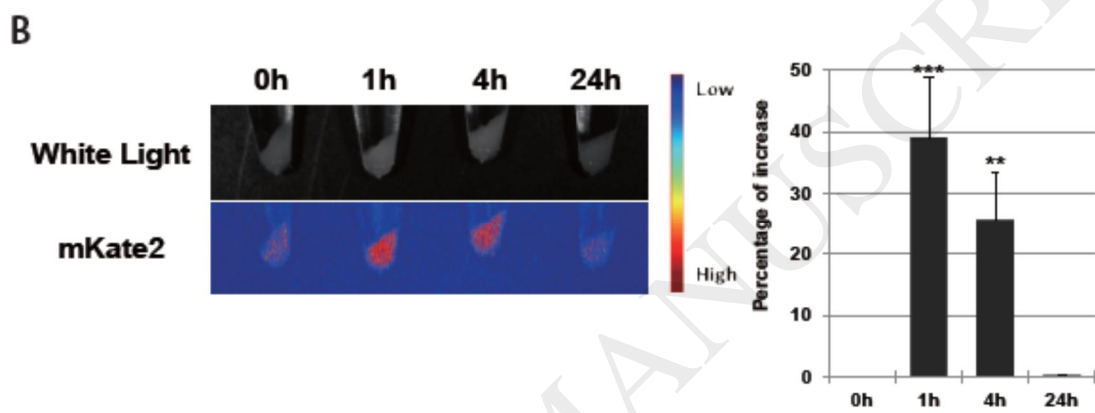
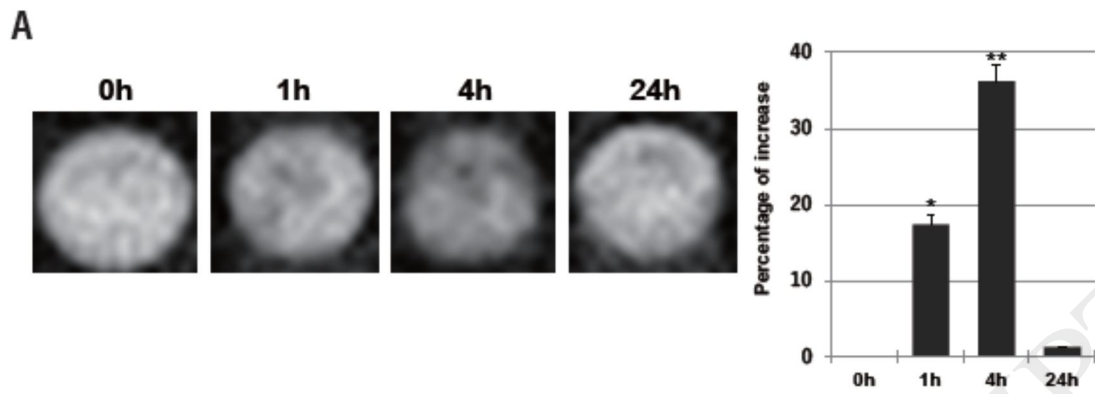
8 treatment. mKate2 fluorescence was measured and the percentage increase in red

9 fluorescence is summarized in a graph. $**P < 0.01$, $***P < 0.001$ compared to that at 0 h. (C)

10 Intracellular iron concentration was measured from the cell pellets and the percentage

11 increase in iron concentration is summarized in a graph. $**P < 0.01$, $***P < 0.001$ compared

12 to that at 0 h.



1

2